ELSEVIER

Ultramicroscopy 56 (1994) 241–252

ultramicroscopy

Analysis of transient structures by cryo-microscopy combined with rapid mixing of spray droplets

John Berriman, Nigel Unwin

MRC Laboratory of Molecular Biology, Hills Road, Cambridge, CB2 2QH, UK

Received 15 June 1994

Abstract

A simple method to determine transient conformations of biological molecules is described. The two reactants (e.g. protein complex and ligand) are mixed rapidly by the coalescence of spray droplets containing one component, with a thin, grid-supported aqueous film containing the other. The transient state is then trapped by rapid freezing, and investigated later by cryo-microscopy. Images of conformations associated with reaction times of 1–100 ms can be achieved by adjusting the delay between the droplet impact and freezing. The droplets (typically 1 μm in diameter) are propelled onto the grid by an atomizer spray. It is shown that the droplets impinging on the liquid film spread rapidly over its surface under the influence of surface tension, and only weakly disturb the underlying film, partially displacing its contents away from the point of impact. Experiments with sprayed salt solutions, using vesicles derived from erythrocytes as micro-osmometers, indicate that rapid mixing occurs both through the film and laterally, by diffusion. The spraying process does not produce any detectable concentration changes due to drying in either the droplets or the film, and the method is applicable to high-resolution imaging.

1. Introduction

It is often necessary to determine the structures of the transient conformations of biological molecules or complexes to obtain a clear understanding of how they work. Time-resolved X-ray crystallographic and solution scattering methods have been developed for this purpose and applied to a limited range of specimens [1–4]. To induce structural change(s), chemical or electrical stimuli, light, or fluctuations in temperature are used, and an important requirement is to initiate the reaction simultaneously throughout the system. Synchronous activation by chemical reagents (effectors or substrates) may be obtained by rapid mixing of the reactants or by illumination of photolabile caged compounds.

Detection and analysis of transient structures can also be carried out by cryo-electron microscopy, using the rapid freezing step involved in preparing the samples to trap a transient state, activated in advance [5]. This approach, combined with prior photolysis of photolabile nucleotides, was used to investigate the interaction of actin filaments with myosin subfragment 1 [6]. However, the application of photolysis methods is limited, depending on the availability of caged compounds having adequate quantum yields and photolysis rates, and may be inappropriate if trace amounts of the breakdown products, or the highly

SSDI 0304-3991(94)00113-8

reactive by-products, are sufficient to modify the specimen. Also, there are likely to be heating problems caused by absorption of the incident light by the metal of the microscope support grid, since this is contacted by only very small volumes of fluid. The use of tuneable lasers may optimise the efficiency of release, but the sensitivity of the specimen to photolytic damage remains a concern.

An alternative approach to flash photolysis would be one in which the activating ligand, or other interacting component, is simply sprayed onto the grid-supported aqueous film on its way to being frozen. With such a technique, the reaction time could be varied by adjusting the delay between the spraying and the freezing, and it should be possible to achieve reaction times down to 1 ms. We describe here an apparatus combining spray-mixing with rapid freezing, which is designed to achieve very short reaction times. We investigate the technique by observing the behaviour of marker particles and also microvesicles, which alter their shape rapidly (within 2 ms) when exposed to sprayed salt solutions. The potential of this approach to reveal conformational changes induced by ligands on fast-acting molecules, such as ion channels, is demonstrated by high-resolution images obtained from sprayed acetylcholine receptor tubes.

2. Methods

2.1. Specimen preparation

2.1.1. Erythrocyte microvesicles

200 ml of packed human red blood cells were incubated in a calcium-containing Tris-buffered saline with a 2 μm ml^{-1} concentration of the ionophore A23187 [7] (Sigma) at 37°C for 2 h. The cells were removed by low-speed centrifugation and the supernatant spun for 30 min at 30 000 g. The red pellet was covered by a light layer of ghost membranes. These were removed and the haemoglobin containing microvesicles were resuspended into isotonic saline using a pipette. Different concentrations of NaCl, up to 1.0M, were sprayed onto grids to which microvesicles had been previously applied, using 2 mg ml^{-1} ferritin (Sigma) as a marker.

2.1.2. Acetylcholine receptor tubes

Preparation of *Torpedo* acetylcholine receptors crystallised on the surfaces of tubular vesicles was as described previously [8]. The tubes were grown and kept in 100mM sodium cacodylate, pH 6.8. The spray solution consisted of 100mM acetylcholine chloride and 2 mg ml^{-1} ferritin, pH 6.8.

2.2. Apparatus for spray-freezing

The freezing device (Fig. 1a) was a standard guillotine-type plunger [9] in which the electron microscope grid, mounted on forceps, was released with a footswitch and allowed to drop by free-fall from a height of a few centimetres above the surface of liquid-nitrogen-cooled ethane. The surrounding environment was enclosed and maintained at a temperature of 4–8°C and at a humidity close to 100%.

An atomizer was selected that would generate a concentrated mist of small (~ 1 μm) droplets from a minimal volume of liquid. The best of many tested (Hampshire Glass, Southampton, UK) contained a small internal jet (0.5 mm diameter) which blew across a rising venturi onto a 4 mm glass sphere (Fig. 1b). The sample could be loaded through a sealable inlet and this allowed a controlled rise of gas pressure during use. A "Gilson Tipac-Yellow" pipette tip, cut to give a final orifice of 3 mm diameter, was fitted to the glass outlet. This tapered nozzle had the effect of focusing the droplets into an area the size of the electron microscope grid.

The atomizer spray was mounted next to the plunger so that droplets emanating from it would intercept the grid at a set distance above the ethane surface (Fig. 1b), depending on the reaction time required. The atomizer was connected through a solenoid valve to a nitrogen cylinder giving a pressure which could be varied between 0 and 2.5 atmospheres. The timing was controlled by using a fibre optic photoswitch (Omron; E3S-X3CE4/E32-DC200) to trigger a pulse generator (Philips PM5704). This was operated in single-

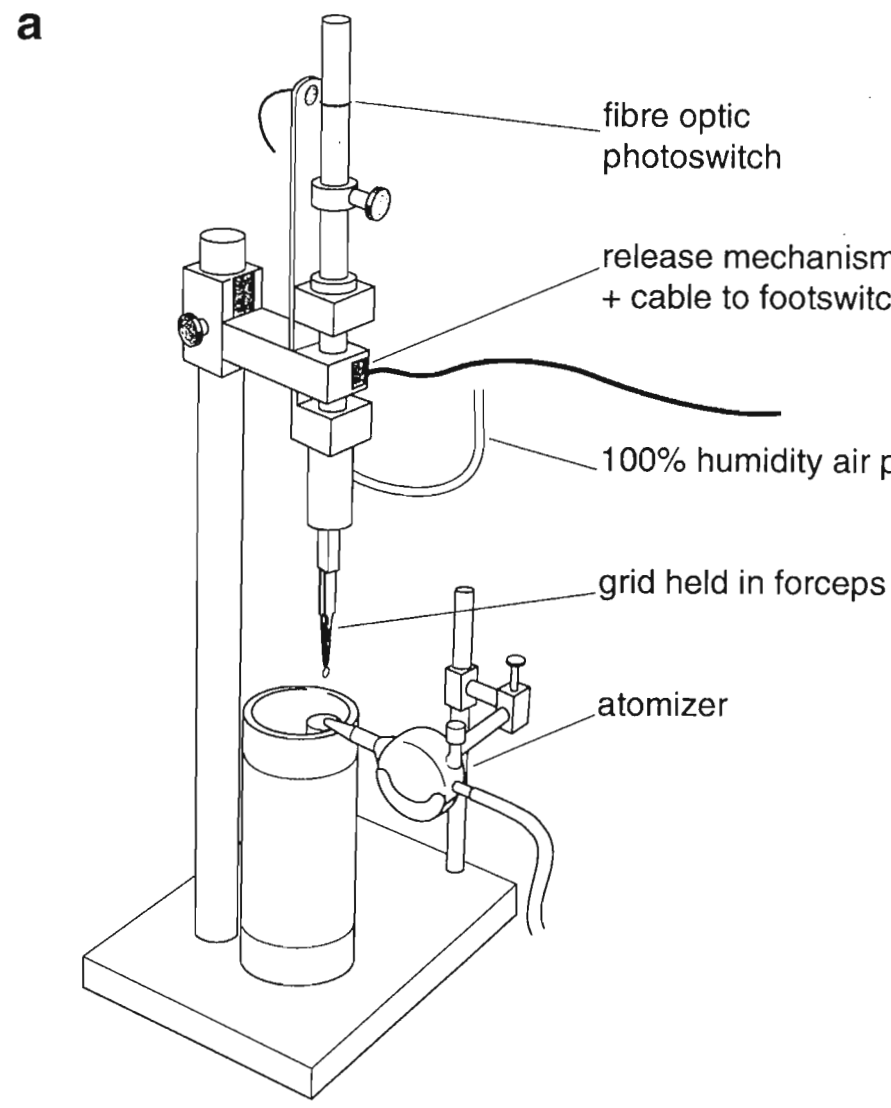

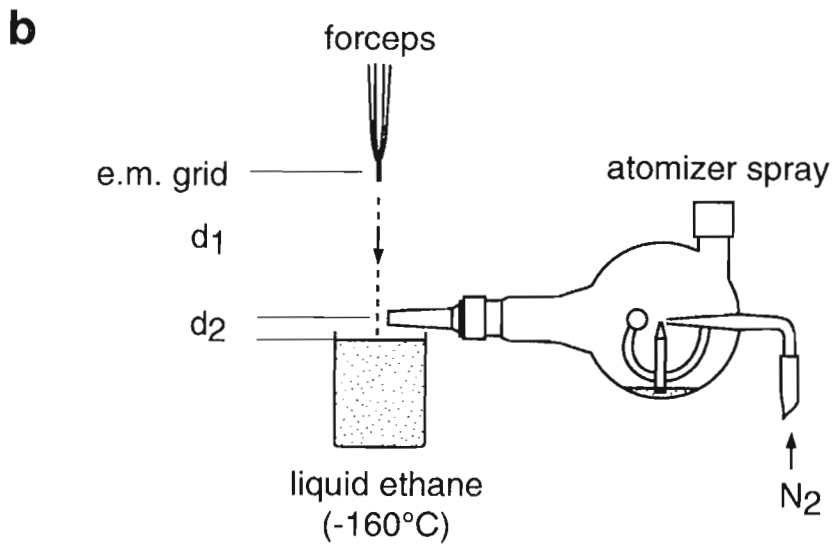

Fig. 1. (a) Spray-freezing apparatus, consisting of a guillotine-type plunger and an atomizer spray. The plunger is released by a footswitch, and the movement activates a fibre optic photoswitch, which in turn triggers the opening of a solenoid valve for nitrogen gas (1.6 bar) to set off the spray. To prevent frosting of the nozzle the liquid-nitrogen-cooled ethane and Dewar are moved into place just before spraying. The whole apparatus is enclosed within a high-humidity chamber. (b) Details of the atomizer spray. The electron microscope grid is held in a pair of forceps at a fixed distance (d_1) above the nozzle of the atomizer, which is at a fixed distance (d_2) above the surface of the liquid ethane. After applying the specimen to the grid, and blotting off the excess solution, it is allowed to drop by free-fall into the ethane.

pulse mode and initiated a normal TTL signal which was used to open the gas solenoid valve (Lucifer, Geneva; Cat. No. 121A-01, 1/4″ bore) via a control box (MRC-LMB). The control box incorporated a variable timing delay circuit and a switch to trip manually a burst of gas without the plunger having to fall. This allowed priming of the atomizer with two or three bursts just before use.

The best generation of small droplets was obtained when the nitrogen gas was supplied to the atomizer in short (60 ms) bursts, and at 1.6 atmospheres (see Results). If the burst was applied for much longer times large droplets would accumulate on the surface of the nozzle and be blown through in subsequent operations, thereby "flooding" the grid with too much material for observation. Another advantage of spraying in short bursts was that the amount of aerosol in the high-humidity chamber could be kept very low, avoiding possible premature reaction of the sample with components in the air.

2.3. Electron microscopy

Samples were applied in 5 μl aliquots to holey carbon films. These films had been prepared by glow-discharge in amylamine vapour [10] and were supported on rigid grids (300 mesh copper, Maxtaform, Graticules Ltd., UK). Excess solution was blotted off the grids, which were then released to fall past the atomizer nozzle into the liquid ethane. For the acetylcholine receptor tubes, the blotting was done from the side opposite to that on which the specimen was applied [11].

Grids were pre-aligned to ensure that they would pass centrally with respect to the nozzle of the atomizer, and the correct distance from it. The atomizer was also primed with two or three bursts blown onto a filter paper, after raising the grid to the release position. The liquid ethane container was then moved into position below the nozzle. The grid was blotted and the footswitch was operated to release the plunger and activate the spray.

Low-dose electron micrographs of the spray-frozen specimens were recorded at underfocus values between 1 and 2 μm, and at an operating voltage of 120 kV, using a Philips EM420 electron microscope equipped with a low-dose kit and an auxiliary twin-bladed anticontaminator. The samples were maintained at ~ -170°C in the microscope, using a Gatan 626 cold stage.

3. Results

3.1. Operating conditions

In a typical experiment, the plunger was released with the grid 35 mm above the nozzle outlet (d_1 in Fig. 1b), which was mounted 4 mm above the surface of the ethane (d_2). Simple calculation shows that under free-fall this arrangement would lead to a delay of about 5 ms between spray impact and immersion of the grid in the liquid ethane. The additional reaction time

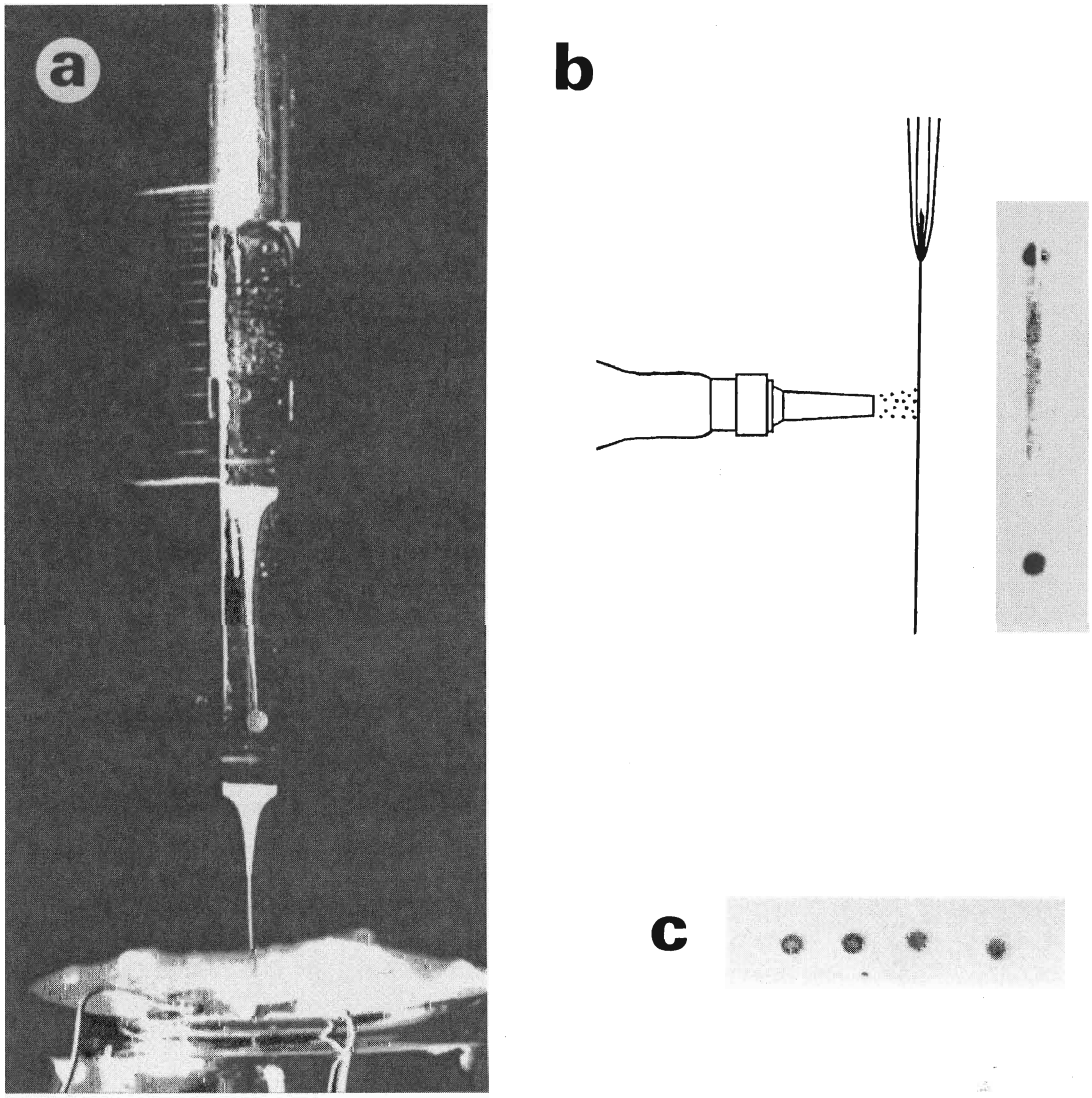

Fig. 2. (a) Stroboscopic measurement of the plunging speed. A wire was attached to the plunger to provide a positional marker and the plunger was allowed to fall while being photographed using a strobe-light flashing every 5 ms. The time marks indicate a velocity of 1 m s^{-1} after a drop of 40 mm. (b) Use of ink to investigate spray characteristics. A strip of filter paper was held in the tweezers and ink was sprayed out of the atomizer marking the starting position (lower spot). The plunger was then released and the spray produced a streak starting after about 50 ms and continuing through the passage of the tweezer-tip and onto the end of the fall (upper spot). The diagram shows the tweezers and paper after the plunger had travelled halfway. (c) Effect of distance on the distribution of droplets in the spray. Ink sprayed onto filter paper indicates that the droplets are concentrated around the perimeter of the jet as it leaves the nozzle, but that further away the distribution is more uniform. The sprayed ink is shown (left to right) for 1, 2, 3 and 4 mm separations between the nozzle and the paper. The optimal setting for small droplets was at 2–3 mm.

following immersion in the ethane is less than 0.1 ms [12], due to the very fast freezing rate associated with the production of amorphous ice. It was necessary to prove that the plunger was not slowed by friction and a set of stroboscope images were recorded of its operation (Fig. 2a). These showed a highly reproducible and almost frictionless fall of the plunger, accelerating to 1 m s^{-1} after a 40 mm drop.

The properties of the spray were explored by using fountain pen ink sprayed onto a strip of filter paper as it fell past the nozzle (Fig. 2b). The streaks produced on the paper helped to show that both grid and spray were intersecting. The spray lasted the duration of a 60 ms burst, but its emergence was delayed by about 50 ms while the pressure built up in the piping and atomizer chamber. Since the grid took 80 ms to fall to the level of the nozzle it passed roughly through the middle of such a burst. By adding an electronic delay it was possible to have the grid passing through the start of the burst, but this did not reveal any advantages.

Other experiments with ink showed that the droplets were concentrated near the perimeter of the spray at the nozzle outlet, but became more uniformly distributed further away (Fig. 2c). A tintometric method was used to measure the amount of ink carried in each 60 ms burst, and the average volume was found to be 0.1 μl. The gas volume passing through the nozzle in the burst, measured by collection over water in a trough, was 20 ml. The water content of the spray was therefore 5 g m^{-3}, similar to that present in storm-clouds [13]. Typically, the grid takes about 3 ms to pass through the spray. As this is 1/20 of the duration of the burst, the volume of dispersed solution available to the grid in transit was about 5 nl. If this were to be evenly distributed over the surface of the grid it would add almost a micrometre to the film thickness. In practice, there was a very large variation in thickness over the frozen grid because most of the liquid volume in the spray was carried by the largest droplets.

The velocity of the spray issuing from the nozzle, according to the above measurements, is

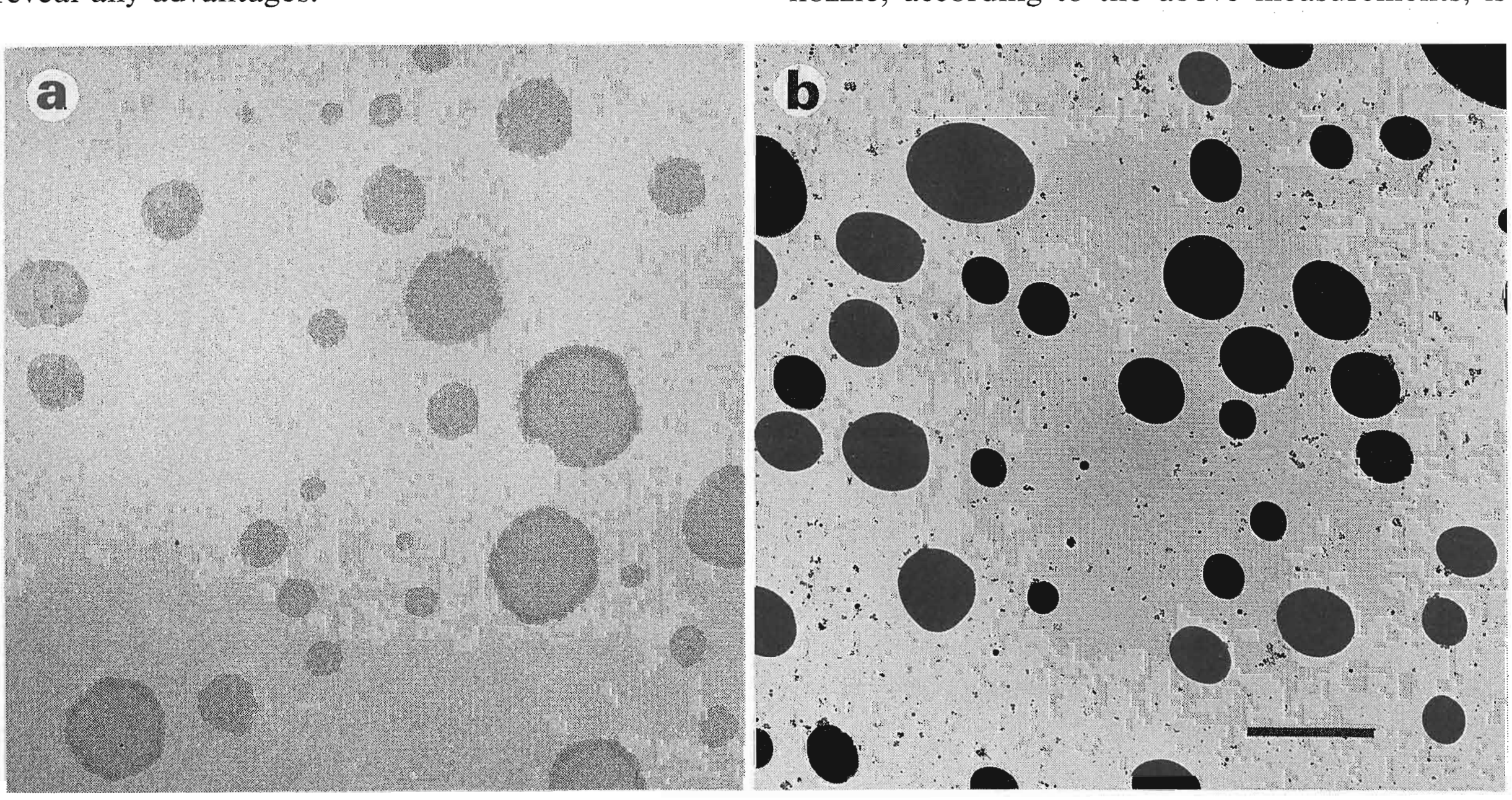

Fig. 3. Size and distribution of spray droplets. (a) A 2 mg ml^{-1} solution of ferritin was sprayed onto a hydrophobic grid under optimal spraying conditions (see text) and allowed to dry before examination by conventional electron microscopy. Circular patches of closely packed ferritin molecules are visible. (b) The same conditions as in (a) except that the sprayed droplets were frozen 5 ms after landing on the hydrophobic surface. The dried and the frozen droplets have similar dimensions in the plane of the grid, indicating that the dried droplets provide a good representation of the extent of the droplets as they impinged on the surface. The scale bar represents 2 μm.

~ 50 m s^{-1}. This high velocity did not appear to damage the carbon support or to flex significantly the thick Maxtaform grids as they passed through the spray. However, atomizers with wider internal jets (~ 1 mm diameter) generated stronger sprays which did damage the support film. The application of lower pressures reduced the force, but the droplets produced were then larger than with the narrower jet and higher pressure.

3.2. Characterisation of the spray droplets

Variables affecting the size and distribution of the droplets were evaluated by electron microscopy using a 2 mg ml^{-1} ferritin sample and the standard plunging distances ($d_1 = 35$ mm, $d_2 = 4$ mm). Droplets impinging on untreated hydrophobic carbon films left patches on the surface when air-dried (Fig. 3a). These dried patches corresponded roughly to the original droplet sizes since they had about the same dimensions in projection as the hemispherical "beads" made by droplets frozen after impinging on the same films (Fig. 3b). Examination of the dried patches therefore provided a simple means to assess the different atomizers and the operating parameters. The number of ferritin particles in the dried patches also allowed the airborne volumes of the droplets to be estimated (a 2 mg ml^{-1} solution contains ~ 2000 ferritin particles μm^{-3}). The smallest droplets, containing ~ 100 ferritin particles in the patches, were only ~ 0.5 μm diameter, more typical droplets had a diameter of 1–2 μm.

The gas pressure and the distance of the grid from the outlet of the nozzle were found to be important in affecting the size and distribution of the droplets. The minimum droplet size occurred at a pressure of about 1.6 atmospheres and with the grid as close as was practical to the nozzle outlet: a distance of 2–3 mm was convenient, and also maximised the density of droplets due to the focusing.

3.3. Spreading and mixing of droplet contents with aqueous films

Droplets impinging on carbon films made partially hydrophilic by glow discharge in amylamine vapour [10], or even completely hydrophilic by glow discharge in air, were observed to spread by various amounts, depending presumably on the different contact angles made by the droplets with the different surfaces. Droplets impinging on a thin liquid film might be expected to spread as on a hydrophilic surface, with a rapid mixing of components occurring at the same time due to diffusion both normal to and in the plane of the film. We investigated the spreading/mixing effects of both small particles and ions with the aqueous film.

3.3.1. Small particles

To examine the movement of small particles, a solution containing 2 mg ml^{-1} ferritin and 0.5 mg ml^{-1} tobacco mosaic virus (TMV) was sprayed onto a thin film containing 10 mg ml^{-1} turnip yellow virus (TYMV), supported by a holey carbon grid. The TMV was used as an essentially non-diffusible marker to indicate the extent of the spreading droplet, and the TYMV as a marker to indicate displacement of contents within the aqueous film. Fig. 4 shows a region where the ferritin/TMV-containing droplet has been frozen

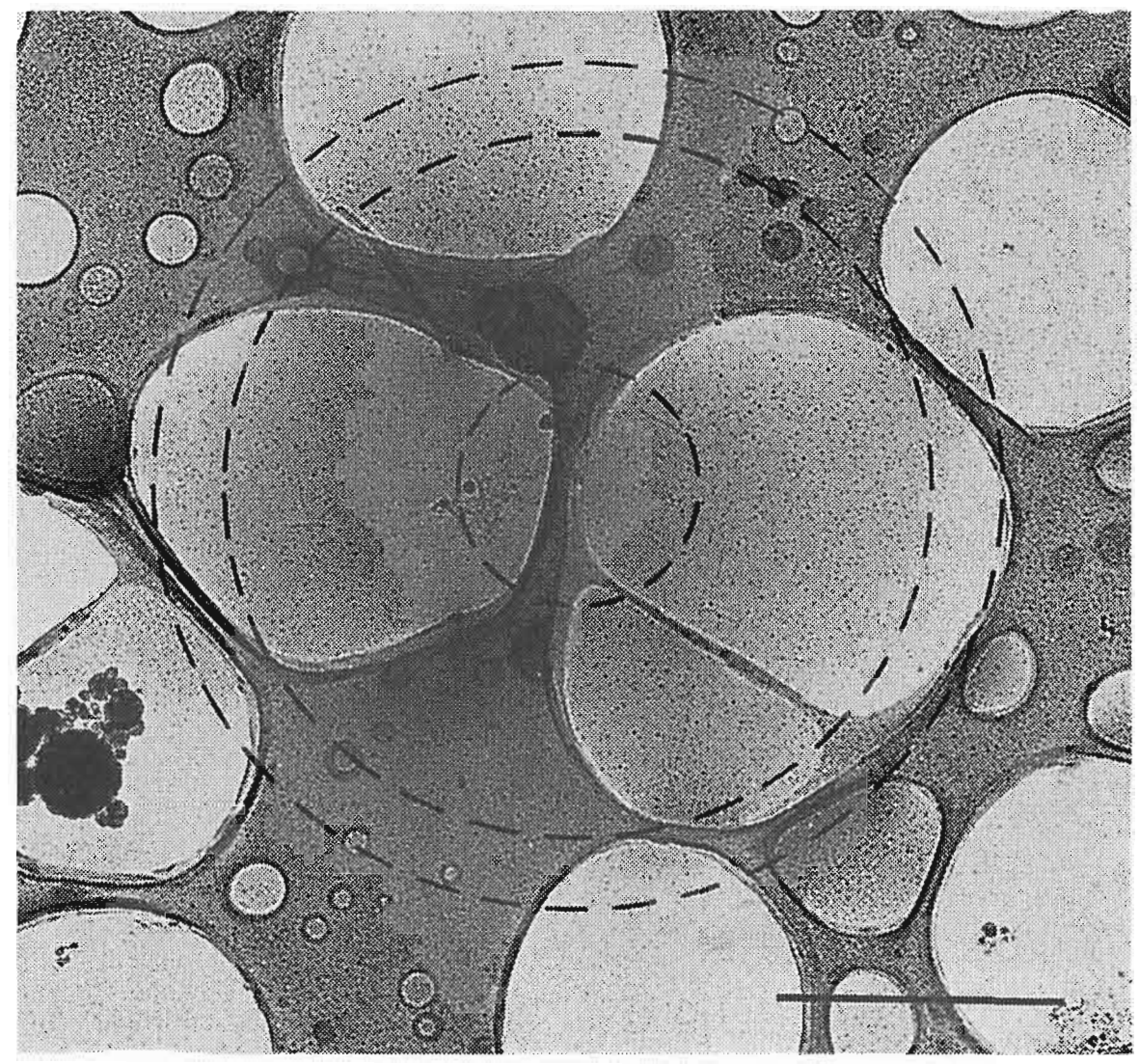

Fig. 4. Image of a partially spread droplet containing ferritin and TMV on the surface of a thin aqueous film containing TYMV. The small circle indicates the diameter of the droplet as it would have been in the spray jet. The intermediate and largest circles indicate respectively the extent of the TMV and the ferritin particles, as determined from higher magnification images. Scale bar: 2 μm.

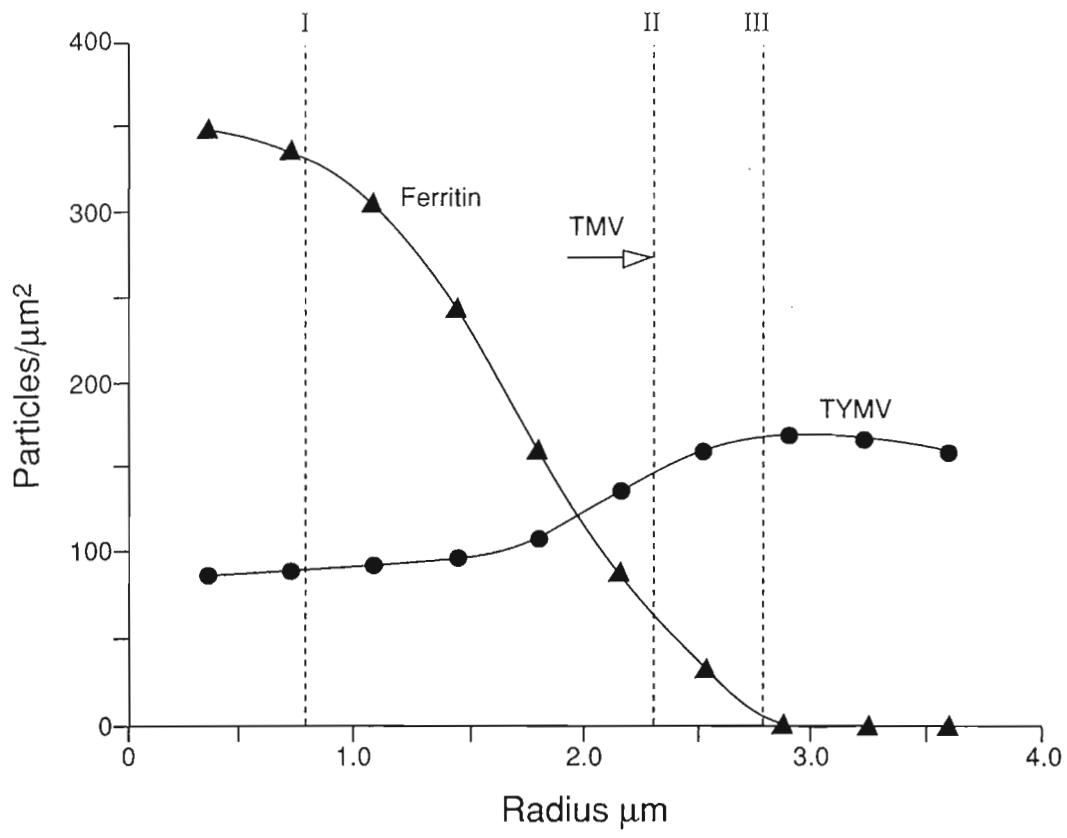

Fig. 5. Graph of the numbers of ferritin (triangles) and TYMV particles (circles) in concentric zones about the point of contact of the droplet in Fig. 4. Ferritin (and TMV) particles were in the spray solution; TYMV was on the grid. The vertical broken lines (I, II and III) correspond to the concentric rings in Fig. 4, and indicate, respectively, the original diameter of the droplet, the radial extent of TMV particles, and the radial extent of the ferritin. The fall-off in the number of ferritin particles away from the point of contact is partly due to the fact that the spreading droplet decreases in thickness away from this point, and is influenced by diffusion (see text). The increase in the number of TYMV particles away from the point of contact indicates that some of the underlying film is pushed outwards by the spreading droplet.

after spreading for 5 ms over the TYMV-containing film. The inner circle shows the original size of the droplet (1.6 μm diameter, estimated by counting the total number of ferritin particles), the intermediate circle the extent of the TMV, and the outer circle the extent of the ferritin.

The resulting distribution of particles was analysed by dividing the image in Fig. 4 into 10 concentric zones having equal radial increments. The number of ferritin, TMV and TYMV particles were counted in each zone, using a collage of higher magnification images (not shown). These values were then used to plot particle concentrations (number per μm^2) as a function of distance from the centre (Fig. 5). Thus, from the extent of the TMV particles, the droplet had spread out to a radius of 2.4 μm (i.e. to 3 $\times$ its original diameter). There was also a lowered concentration of TYMV particles "underneath" the spreading droplet, indicating that the film contents had been partly pushed outwards at the same time.

The ferritin particles extend beyond the TMV particles by about 0.5 μm (Figs. 4 and 5). This finding can be accounted for by considering that the diffusion coefficient, D, of the ferritin is $\sim 10^{-7}$ cm^2 s^{-1} [14], leading to a calculated diffusion distance ($2\sqrt{Dt}$) of 0.45 μm, and that TMV (diffusion coefficient $\sim 10^{-9}$ cm^2 s^{-1} [14]) would diffuse ten times less over the same period. The ferritin particles should therefore be present a small distance beyond the TMV because of their more rapid diffusion.

3.3.2. *Ions*

The erythrocyte microvesicles used for detecting ion movement (see Methods) were mostly

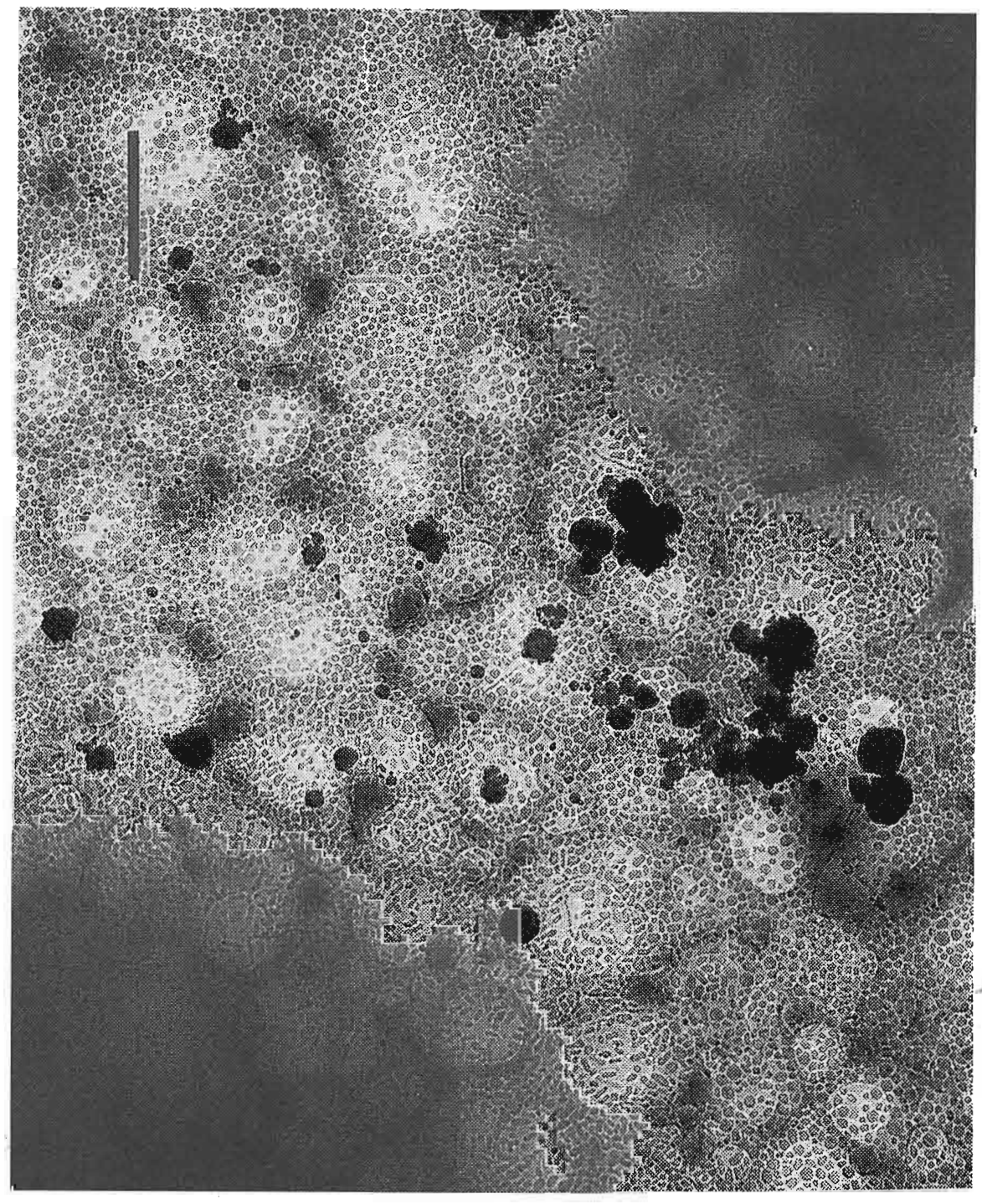

Fig. 6. Changes in ion concentration detected by shape changes in erythrocyte vesicles. The vesicles in 0.15M NaCl were applied to an air glow-discharged holey carbon film and blotted. A 1.0M NaCl solution containing 2 mg ml^{-1} ferritin was sprayed onto the grid, which was frozen after 10 ms. The low-magnification image shows where two droplets have landed (darker areas) and caused shape changes to the spherical vesicles. The scale bar represents 2 μm.

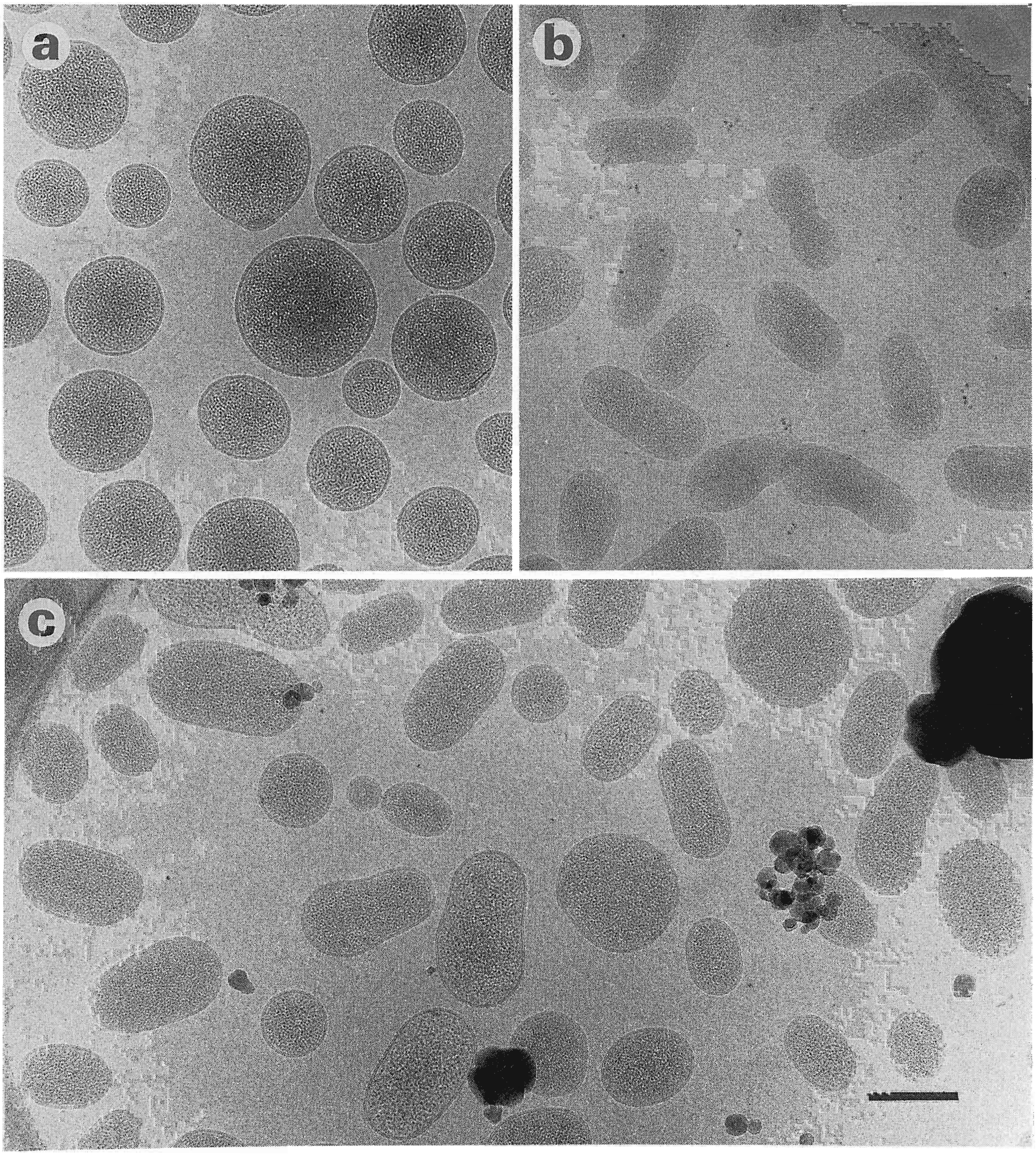

Fig. 7. Erythrocyte vesicles in different ionic environments. Areas selected from the sample in Fig. 6 are shown at higher magnification. (a) Away from the areas of the sprayed salt solution the vesicles are spherical and have a single membrane enclosing densely packed haemoglobin molecules. (b) Within the area of impact of the droplets (indicated by the presence of ferritin particles) the vesicles have become ellipsoidal or "sausage-shaped". (c) At the edge of the droplet, beyond the ferritin, the diffusing salt also causes the vesicles to become ellipsoidal in shape. A few ferritin particles are seen on the left of this picture (towards the droplet). The scale bar represents 0.1 μm in all images.

single membrane bound spherical vesicles. They were typically 100–200 nm diameter and loaded with haemoglobin. The vesicles functioned as micro-osmometers because their shape changed from spherical to ellipsoidal when they were incubated in NaCl solutions above isotonic levels (~0.15M NaCl). Control experiments, applying very short delays between spray impact and freezing, showed that this shape change was detectable after a rise from 0.15M to 0.3M salt within 2 ms.

Figs. 6 and 7 show the appearance of the vesicles on the grid, after spraying with a 1.0M NaCl solution containing ferritin marker particles and applying a 10 ms delay between spray impact and freezing. The predominantly spherical vesicles (Fig. 7a) became ellipsoidal within the region of impact of the droplets (Fig. 7b) and in neighbouring regions (Fig. 7c). The shape change, measured from the ratio of the major to minor axes of the ellipsoidal vesicles, was plotted for a large number as a function of the distance from the centre of the droplets. The extent of the ferritin was checked with higher-magnification images. The averaged measurements for the vesicles around four spray droplets (Fig. 8) revealed that the salt ions caused a shape change up to ~3 μm beyond the ferritin marker particles. This finding is consistent with the fact that an ion (diffusion coefficient $\sim 10^{-5}$ cm^2 s^{-1} [15]) would be expected to diffuse over a distance ($2\sqrt{Dt}$) of about 6 μm in 10 ms.

As the vesicles behaved as osmometers it was possible to confirm that no significant drying had been caused by the burst of gas over the surface of the grid. If the humidity of the gas had been much below 100% it was likely that water would have been lost from the grid through forced evaporation. The fact that the vesicles on the grid away from the droplets were still spherical (Fig. 7a) showed that this kind of drying was not detectable. An alternative source of evaporation, which may occur even at 100% relative humidity, is the distillation of water out of small droplets due to the effects of surface tension [16]. However, the vesicles in small vesicle-containing droplets, which had been sprayed onto air glow-discharged carbon films and rapidly frozen, were still spherical (data not shown), indicating that there was no appreciable concentration change within droplets over the time-scale of the burst.

3.4. Application to high-resolution structural studies

It was possible that the disturbances associated with the rapid spreading and mixing of the spray droplets would lead to distortions of the specimen, and thereby prevent high resolution imaging. Experiments with the fragile, but well characterised acetylcholine receptor tubes [17,18] demonstrated that such disturbances are unlikely to present a serious problem. Fig. 9a shows an image of an acetylcholine receptor tube obtained after spraying with a solution containing ferritin marker particles and acetylcholine. The delay between spraying and freezing had been set to 5 ms in order to induce the open-channel form of the receptor and avoid the rapid transition to the desensitised state. The presence of ferritin particles in the image indicates that acetylcholine had reached the receptors, and the overall shape and straightness of the tube indicate that no gross distortions had occurred.

The layer-lines in Fourier transforms of such acetylcholine-activated tubes (Fig. 9b) show strong high-resolution data, indicating that the helical packing of receptors is not disrupted by spraying.

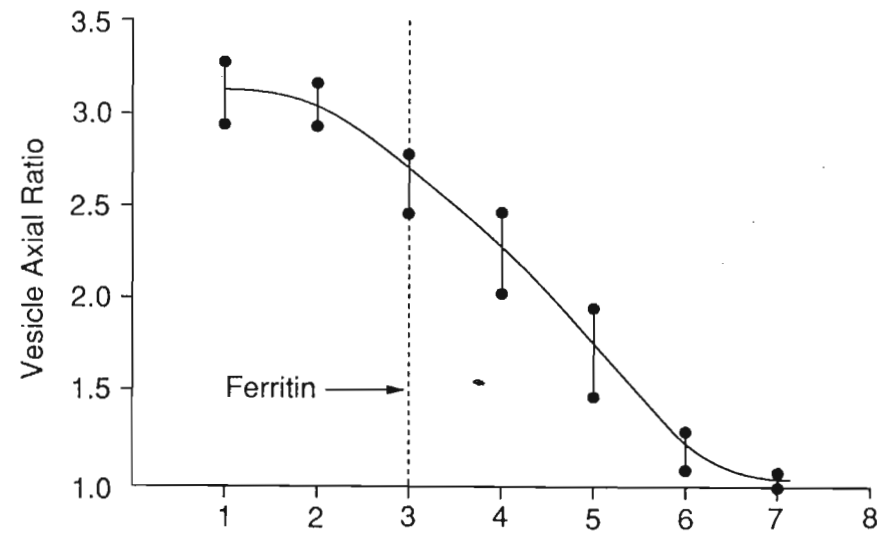

Fig. 8. Movement of ions in the vicinity of spreading salt-containing droplets. The areas around four sprayed droplets (as shown in Fig. 6) were divided into a series of 1 μm wide concentric zones. The axial ratios of the vesicles were measured for a large number of vesicles in each zone and the average values plotted in the graph. A significant effect by the diffusing salt on the shape of the vesicles was found up to about 3 μm beyond the limit reached by the ferritin particles, indicating substantial lateral diffusion of the ions over the 10 ms mixing period.

The transforms have good mirror symmetry, confirming that the tubes are completely embedded in the ice. Transient conformational changes associated with the presence of acetylcholine are evidently too small to be easily detectable by superficial examination of individual transforms. However, with a number of such images, and image averaging [17], it should be possible to determine the nature of the conformational change that opens this channel.

4. Discussion

Studies to detect and analyse rapid conformational changes have so far been confined mainly to X-ray diffraction measurements. However, for several kinds of specimen or system, the cryo-microscopical method described in this paper might have important advantages. First, it would be the most appropriate method to investigate transient conformational changes in membrane proteins

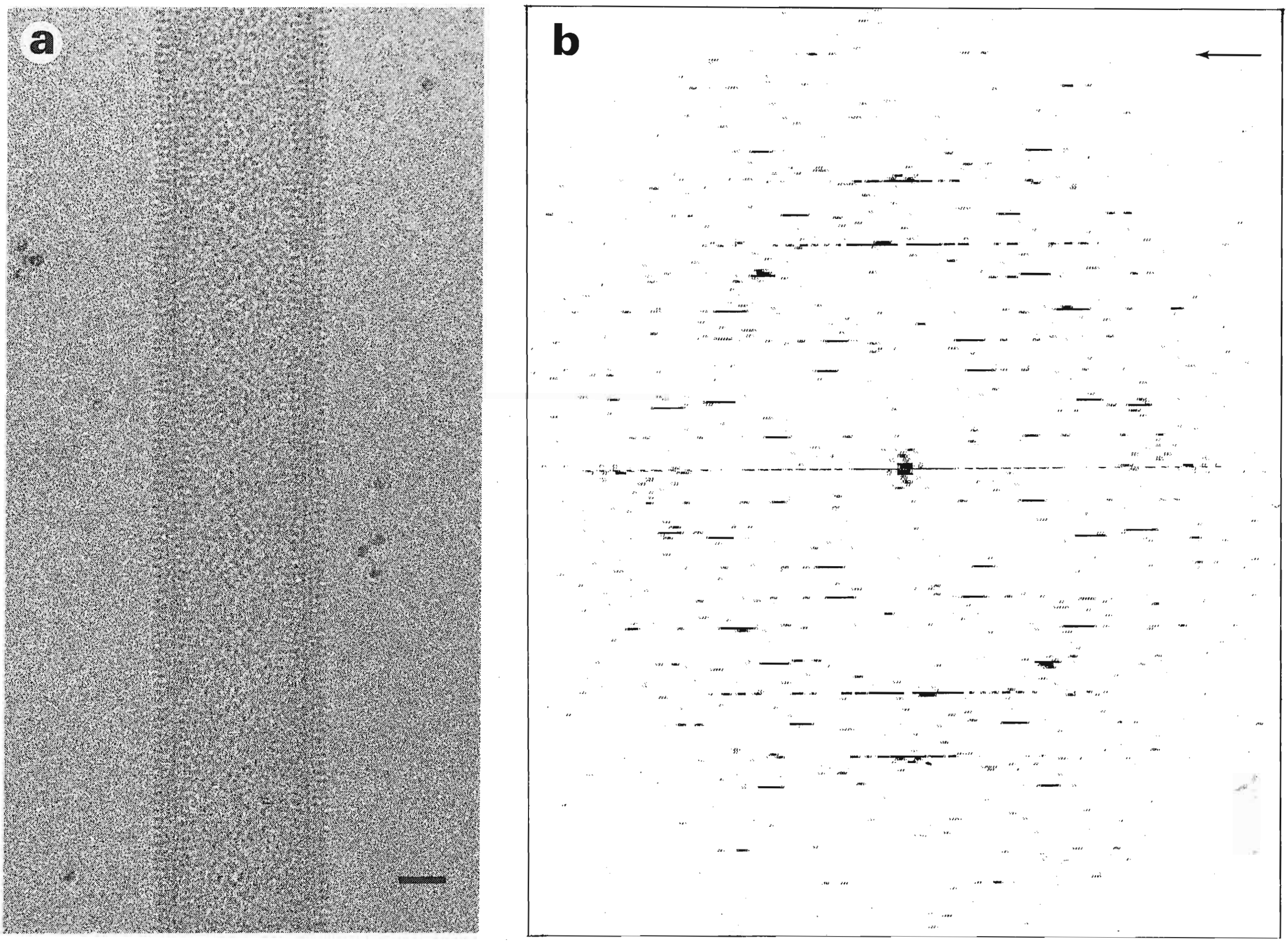

Fig. 9. (a) Image of an acetylcholine receptor tube in a thin film of amorphous ice, after spray-freezing with a solution containing 100mM ACh and 2 mg ml^{-1} ferritin. The delay between spray impact and freezing was 5 ms. The presence of ferritin particles surrounding the tube indicates that this tube was near the point of impact of a spray droplet. (b) Fourier transform computed from a tube of the (−16,6) helical family [18], imaged under the same conditions, at 0.77 μm underfocus. The layer-lines are sharp and predominantly mirror-symmetric, indicating good preservation of the helical symmetry. The arrow points to peaks on the (1,5;14) layer-line [18], which are at a reciprocal spacing of 1/22 $Å^{-1}$. Image processing of such tubes indicates that the Fourier terms extend, as previously [17], to at least 9 Å resolution.

retained in their natural lipid surroundings. Second, the microscope could be used to examine a heterogeneous mixture of biological molecules, or complexes because one is observing the specimens on an individual basis. The images should reveal small localised effects, which would be averaged out if a three-dimensional crystal or homogeneous solution were used. Third, the spraying method facilitates a wider range of reaction possibilities than does the use of flash photolysis, and may even allow study of the behaviour of molecules under the influence of concentration gradients associated with a spreading drop.

As a guide to developing the spray-freezing method the erythrocyte vesicles have provided a clear and simple example of a fast-acting test object. The red cell membrane is known to contain a water channel [19], and it is interesting to speculate that the speed with which water exits from the vesicles in a hypertonic environment is dependent on this protein. However, calcium ionophore treatment modifies the composition of the erythrocyte membrane [7]; the high water permeability of the vesicles may therefore depend on other factors.

The free-fall freezing device described here allows delays of 1–100 ms between spray impact and freezing to be achieved simply by adjusting the levels d_1 and d_2 (Fig. 1b). However, longer delays could readily be obtained by controlling the rate of plunging. The methodology would benefit substantially from the development of sprays having finer dispersions of even smaller droplets. This would facilitate a more uniform mixing of the reactants on the grid, and lead to greater accuracy in the time delays and concentration levels achieved. Also the larger droplets frequently either cover regions of a grid square with too much ice, or disrupt the liquid film across the holes in the carbon. The atomizer design described has been used in electron microscopy for a long time [20], and it is likely that other types of sprays could be adapted to give sufficient small droplets for this application. For example, it might be possible to generate a high enough aerosol density of monodisperse sub-micron droplets by electro-spraying [21,22]. This depends on charge rather than a jet of gas to break up the liquid into the fine droplets and transfer it to a target. The efficiency of this kind of deposition should be high and, because of the very small energy involved, the sample will be minimally disturbed.

High-resolution maps are normally required to provide reliable descriptions of conformational changes effected by ligands, and hence to make significant contributions to what we know of molecular function. However, secondary structure in proteins can now be visualised by image analysis of suitably crystalline specimens [17,23,24] and sub-nanometer resolution three-dimensional maps of transient states should become available by the approach described in this paper. There was the possibility that mechanical factors could disorganise samples for high-resolution work, since the impact of the droplets on the liquid film was shown to cause some dilution of the film contents (Fig. 5). However, the orientations of the ellipsoidal vesicles within the impacted regions were random (Fig. 7b), indicating minimal disturbance associated with the spreading, and acetylcholine-activated receptor tubes could be found which were as well preserved (Fig. 9) as they are without spray-activation.

5. Conclusions

In this study we have investigated the potential of combining spray-freezing with cryo-microscopy to determine transient conformations of biological molecules. Rapid mixing of the reactants was obtained by spraying droplets containing one component onto a grid-supported aqueous film containing the other; rapid freezing halted the reaction and trapped the transient state: cryo-microscopy allowed evaluation of the structure. We investigated factors which affected the size, density and distribution of the droplets, and also the nature of the spreading and mixing of the impinging droplets with the aqueous film. It was shown that the droplets spread over the surface of the film, only partially displacing its contents away from the point of impact and causing little mechanical distortion to the examined structures.

We demonstrated that this approach is applicable to high-resolution imaging.

Acknowledgements

We are grateful to Chikashi Toyoshima, Chris Raeburn and Dominic Ostrowski for the suggestions and for practical help at various stages in the development of the spray-freezing apparatus. We would also like to thank Michael Moody for the idea of using an osmotic reaction. This research was supported, in part, by a grant (GM41449) from the National Institutes of Health.

References

[1] J. Hadju and I. Andersson, Annual Rev. Biophys. Biomol. Struct. 22 (1993) 467.
[2] M. Kress, H.E. Huxley, A.R. Farquis and J. Hendrix, J. Mol. Biol. 18 (1986) 325.
[3] G. Rapp, K.J.V. Poole, Y. Maeda, K. Guth, J. Hendrix and R.S. Goody, Biophys. J. 50 (1986) 993.
[4] U. Spann, W. Renner, E.M. Mandelkow, J. Bordas and E. Mandelkow, Biochemistry 26 (1987) 1123.
[5] S. Subramaniam, M. Gerstein, D. Oesterhalt and R. Henderson, EMBO J. 12 (1993) 1.
[6] J.-F. Menetret, W. Hofmann, R.R. Schroder, G. Rapp and R.S. Goody, J. Mol. Biol. 219 (1991) 139.
[7] S.D. Shukla, J. Berriman, R. Coleman, J.B. Finean and R.H. Michell, FEBS Lett. 90 (1978) 289.
[8] E. Kubalek, S. Ralston, J. Lindstrom and P.N.T. Unwin, J. Cell Biol. 105 (1987) 9.
[9] J. Lepault, F.P. Booy and J. Dubochet, J. Microscopy 129 (1983) 89.
[10] J. Dubochet, J. Lepault, R. Freeman, J.A. Berriman and J.-C. Homo, J. Microscopy 128 (1982) 219.
[11] C. Toyoshima, Ultramicroscopy 30 (1989) 439.
[12] E. Mayer and G. Astl, Ultramicroscopy 45 (1992) 185.
[13] C.T.R. Wilson, Phil. Trans. Roy. Soc. A 221 (1920) 73.
[14] T.E. Creighton, Proteins: structures and molecular principles (Freeman, New York, 1984).
[15] B. Hille, Ionic channels of excitable membranes (Sunderland, Sinauer Associates, Massachusetts, 1992).
[16] A.G. Bailey, Atomisation Spray Technol. 2 (1986) 95.
[17] N. Unwin, J. Mol. Biol. 229 (1993) 1101.
[18] C. Toyoshima and P.N.T. Unwin J. Cell Biol. 111 (1990) 2623.
[19] G.M. Preston, T.P. Carroll, W.B. Guggino and P. Agre, Science 256 (1992) 385.
[20] M. Reissig and S.A. Orrell, J. Ultrastruct. Res. 32 (1970) 107.
[21] B. Vonnegut and L. Neubauer, J. Colloid Sci. 7 (1952) 616.
[22] G.M.H. Meesters, P.H.W. Vercoulen. J.C.M. Marijnissen and B. Scarlett, J. Aerosol Sci. 22, Suppl. 1 (1991) S11.
[23] R. Henderson, J.M. Baldwin, T.A. Ceska, F. Zemlin, E. Beckmann and K.H. Downing, J. Mol. Biol. 213 (1990) 899.
[24] W. Kühlbrandt, D.N. Wang and Y. Fujiyoshi, Nature 367 (1994) 614.